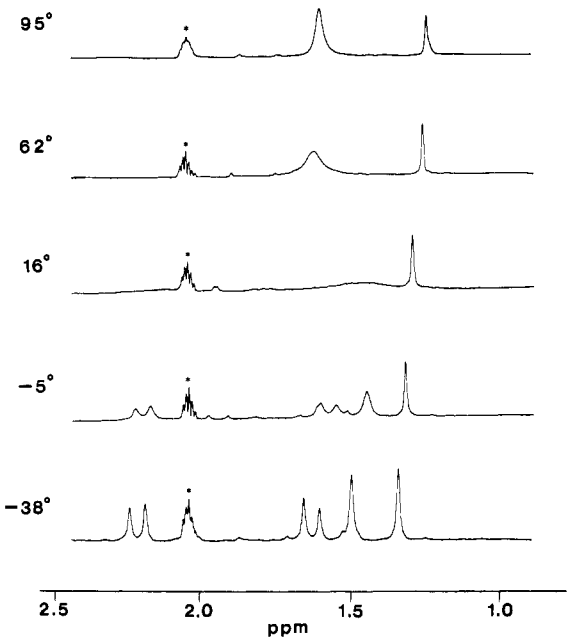

Figure 3. The methylene proton signals of a solution of $Mo_2(NMe_2)_2(CH_2SiMe_3)_4$ in toluene-d_8 recorded at various temperatures in the range −38 to +95 °C and at 220 MHz. The signals arising from toluene-d_8 methyl proton impurities are denoted by an asterisk and reveal a slight loss of resolution in both the high and low temperature limiting spectra shown in this figure. Also to be noted is the slight shift to a higher field of the methylene resonances with increasing temperature.

The variable temperature ^1H NMR spectra of $Mo_2(NMe_2)_2(CH_2SiMe_3)_4$ are particularly fascinating (Figure 3). At 220 MHz and −38 °C, the spectrum is consistent with the adoption of the frozen-out structure shown below. There are three types

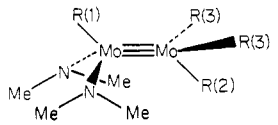

of (trimethylsilyl)methyl groups, R(1), R(2), and R(3); the methylene protons associated with R(3) are diastereotopic and appear as an AB quartet while those associated with R(1) and R(2) appear as single resonances in accord with the existence of the molecular plane of symmetry which contains the anti-C–Mo–Mo–C atoms. There are proximal and distal *N*-methyl resonances. When the temperature is raised, the proximal and distal *N*-methyls coalesce to a sharp singlet as rotation about the Mo–N bonds becomes rapid and the AB quartet collapses and coalesces with one of the methylene proton singlets, leading to a simple 3:1 pattern for both the methylene and methyl groups of the (trimethylsilyl)methyl ligands above 60 °C. This is the first direct observation of rotation about a triple bond which, being cylindrical in nature, should have only a sterically imposed rotational barrier.[6]

This work also provides a direct observation of alkyl transfer between the molybdenum atoms in the dimers. This is evidently a slower process than rotation about the Mo–Mo triple bond, as seen for 1,1-$Mo_2(NMe_2)_2(CH_2SiMe_3)_4$, and it remains to be determined whether alkyl transfer occurs by an inter- or intramolecular exchange process. The isolation of 1,1- and 1,2-$Mo_2(O\text{-}t\text{-}Bu)_2(CH_2SiMe_3)_4$ from differing reactions (see Scheme I) implies the existence of a fairly sizable energy barrier to alkyl transfer in the pure ethanelike compounds. Moreover, when $Mo_2(CH_2SiMe_3)_6$ and 1,2-$Mo_2Br_2(CH_2SiMe_3)_4$ are dissolved together in hydrocarbon solvents, no $Mo_2Br(CH_2SiMe_3)_5$ is formed despite the fact that a ca. 1:2:1 distribution of the hexa-, penta-, and tetraalkyldimolybdenum compounds is formed (a) upon addition of HBr (1 equiv) to a hydrocarbon solution of $Mo_2(CH_2SiMe_3)_6$ and (b) upon addition of $LiCH_2SiMe_3$ (1 equiv) to a hydrocarbon solution of 1,2-$Mo_2Br_2(CH_2SiMe_3)_6$.[7]

Further work is in progress.[8]

(6) Previously we have monitored anti ⇌ gauche isomerization in $Mo_2X_2(NR_2)_4$ compounds, but it has not been possible to establish that this is the effect of a "simple" rotation about the M–M triple bond. See ref 1a and references therein. An estimate for $\Delta G^\dagger$ for rotation about the Mo≡Mo bond in 1,1-$Mo_2(NMe_2)_2(CH_2SiMe_3)_4$ is 14 ± 2 kcal mol^{-1}.

(7) We have been unable to isolate pure $Mo_2Br(CH_2SiMe_3)_5$ because it is extremely soluble in hydrocarbon solvents and is thus not readily separable from $Mo_2(CH_2SiMe_3)_6$. ^1H NMR data for $Mo_2Br(CH_2SiMe_3)_5$ obtained at 220 MHz, 16 °C in toluene-d_8: $(Me_3SiCH_2)_2BrMo$, δ (CH_2) 4.56 (d), 0.66 (d, J = 11.5 Hz); δ ($SiMe_3$) 0.31 (s); $Mo(CH_2SiMe_3)_3$, δ (CH_2) 2.00 (s); δ ($SiMe_3$) 0.26 (s).

(8) We thank the donors of the Petroleum Research Fund, administered by the American Chemical Society, the National Science Foundation, and the taxpayers of the state of Indiana for financial support of this work.

(9) Camille and Henry Dreyfus Teacher-Scholar, 1979–1984.

Malcolm H. Chisholm,*[9] Ian P. Rothwell
Department of Chemistry, Indiana University
Bloomington, Indiana 47405

Received January 29, 1980

Identification of the Enantioselective Step in the Asymmetric Catalytic Hydrogenation of a Prochiral Olefin

Sir:

The use of chiral catalysts to effect the asymmetric hydrogenation of prochiral olefinic substrates with high optical yields represents one of the most impressive achievements to date in catalytic selectivity.[1-3] Especially high optical yields, approaching 100% enantiomeric excess, have been achieved in the hydrogenation of prochiral enamides to the corresponding amides, using homogeneous cationic rhodium catalysts containing chiral phosphine [especially chelating bis(tertiaryphosphine)] ligands (eq 1).[1-5] While various studies have documented the empirical

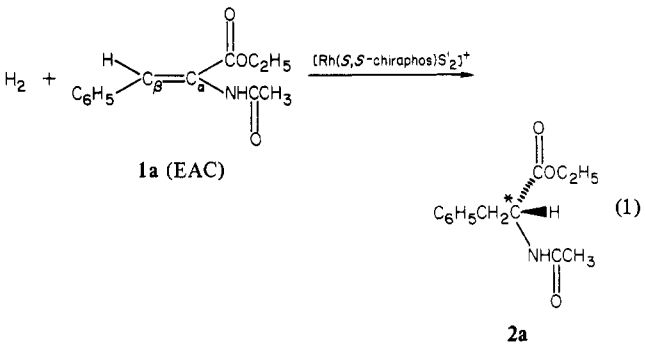

dependence of the rates and stereoselectivities of such reactions on structural features of the catalysts and substrates, an understanding of the origin of these remarkable stereoselectivities and rational approaches to the design of such stereoselective catalysts must rest ultimately upon a mechanistic understanding which

(1) Knowles, W. S.; Sabacky, M. J.; Vineyard, B. D. *Adv. Chem. Ser.* **1974**, *No. 132*, 274.
(2) Kagan, H. B. *Pure. Appl. Chem.* **1975**, *43*, 401, and references therein.
(3) Valentine, D. S., Jr.; Scott, J. W. *Synthesis* **1978**, 329.
(4) Vineyard, B. D.; Knowles, W. S.; Sabacky, M. J.; Bachman, G. L.; Weinkauff, D. J. *J. Am. Chem. Soc.* **1977**, *99*, 5946.
(5) Fryzuk, M. D.; Bosnich, B. *J. Am. Chem. Soc.* **1977**, *99*, 6262.

0002-7863/80/1502-5952$01.00/0

encompasses the *interception and structural characterization* of the stereoregulating intermediates. We report here the results of the first study that directly addresses this theme.

Our observations relate to the hydrogenation of ethyl (*Z*)-α-acetamidocinnamate (EAC, **1a**) in methanol solution, using $[Rh(S,S\text{-chiraphos})S_2']^+$ as catalyst [where *S,S*-chiraphos = (2*S*,3*S*)-bis(diphenylphosphino)butane (**3**)[5] and S′ = solvent, i.e.,

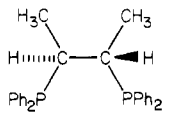

3

CH_3OH] (eq 1). In agreement with earlier findings,[5] we have confirmed that this reaction proceeds with high enantioselectivity, yielding *N*-acetyl-(*R*)-phenylalanine ethyl ester (>95% enantiomeric excess) at 25 °C.

In earlier studies,[6-8] we have concluded that the closely related $[Rh(diphos)S_2']^+$-catalyzed hydrogenation of **1b** (eq 2) proceeds through the mechanistic sequence depicted by eq 3–6 [where MAC = **1b** and diphos = 1,2-bis(diphenylphosphino)ethane].

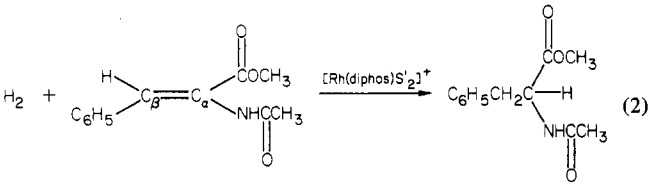

1b (MAC) **2b** (2)

$$[Rh(diphos)S_2']^+ + MAC \underset{k_{-3}}{\overset{k_3}{\rightleftharpoons}} \underset{\mathbf{4}}{[Rh(diphos)(MAC)]^+} + 2S' \quad (3)$$

$$\mathbf{4} + H_2 \xrightarrow{k_4} \underset{\mathbf{5}}{[RhH_2(diphos)(MAC)]^+} \quad (4)$$

$$\mathbf{5} + S' \xrightarrow{\text{fast}} \underset{\mathbf{6}}{[Rh(H)(MACH)(diphos)S']^+} \quad (5)$$

$$\mathbf{6} + S' \xrightarrow{k_6} [Rh(diphos)S_2'] + \mathbf{2b} \quad (6)$$

The intermediates **4** and **6**, whose structures are depicted schematically below, were intercepted and characterized spectroscopically (electronic and NMR) in solution.[7,8] The structure

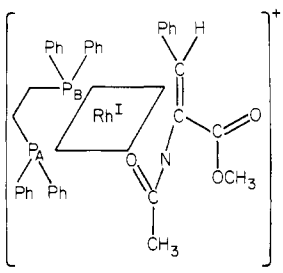

4

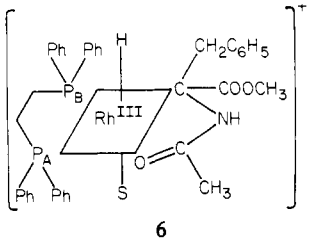

6

of **4** also was determined by single-crystal X-ray diffraction.[7] At temperatures above −40 °C, the second step of the sequence (corresponding to the rate constant k_4) is rate determining.

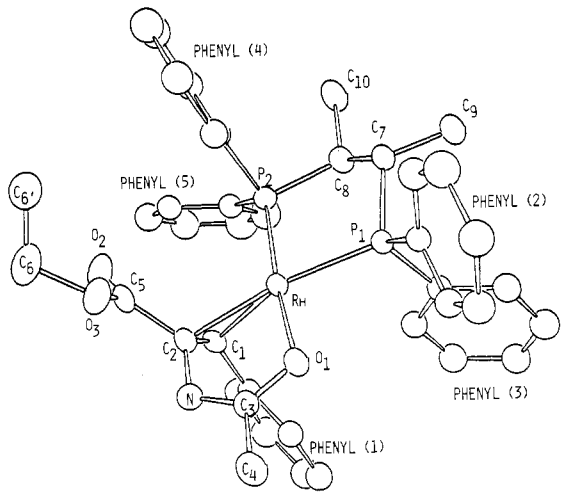

Figure 1. Structure of $[Rh(S,S\text{-chiraphos})(EAC)]^+$. Selected bond lengths (Å): Rh–P_1, 2.289 (2); Rh–P_2, 2.232 (2); Rh–O_1, 2.128 (5); Rh–C_1, 2.197 (8); Rh–C_2, 2.171 (8). Selected bond angles (deg): P_1–Rh–P_2, 83.1 (1); P_1–Rh–O_1, 89.8 (2); P_1–Rh–C_1, 147.3 (3); P_1–Rh–C_2, 167.9 (2); P_2–Rh–O_1, 168.2 (2); P_2–Rh–C_1, 93.1 (2); P_2–Rh–C_2, 109.0 (2); O_1–Rh–C_1, 98.0 (3); O_1–Rh–C_2, 78.0 (3); C_1–Rh–C_2, 36.9 (4).

The essential features of reaction 1 were found to parallel those of reaction 2.[9] Formation of an $[Rh(S,S\text{-chiraphos})(EAC)]^+$ adduct (**7**), analogous to **4**, occurred with an equilibrium constant (determined spectrophotometrically) $K_{eq} = [\mathbf{7}]/[\mathbf{1a}][Rh(S,S\text{-chiraphos})S_2']^+ = 3.5 \times 10^3\ M^{-1}$, similar to that for **4** ($5.3 \times 10^3\ M^{-1}$). The electronic spectrum of **7** [λ_{max} 490 nm (ϵ $1.66 \times 10^3\ M^{-1}\ cm^{-1}$), λ_{min} 440 nm (ϵ $1.46 \times 10^3\ M^{-1}\ cm^{-1}$)] also was similar to that of **4**, as were the NMR parameters of **7**: ^{31}P NMR δ 60.2 (P_A), 72.1 (P_B) ($J_{Rh-P_A} = 154$, $J_{Rh-P_B} = 160$, $J_{P_A-P_B} = 51$ Hz).[7] Only a single diastereomer of **7** in solution could be identified by NMR, and it is concluded that the second diastereomer (which is expected to exhibit a distinguishable NMR spectrtum)[10] must be present to the extent of less than 5%. ^{31}P NMR line-broadening measurements on **7** in the presence of excess EAC confirmed that exchange of coordinated and free EAC was rapid (~3 s^{-1} at 25 °C) and apparently proceeded by a dissociative mechanism (rate independent of the free EAC concentration).

The rate law for reaction 1 also was similar to that previously found for reaction 2, namely $-d[H_2]/dt = k_4'[H_2][Rh(S,S\text{-chiraphos})(EAC)]^+$, with $k_4' = 1.6\ M^{-1}\ s^{-1}$, i.e., about 60 times smaller than the corresponding value of k_4 for reaction 2.[7,8,11] *This rate difference represents the only significant disparity revealed by the various solution measurements on reactions 1 and 2.*

The adduct $[Rh(S,S\text{-chiraphos})(EAC)]^+$ (**7**) was isolated as the ClO_4^- salt by following procedures similar to those previously employed for **4**,[7] and its structure was determined by single-crystal X-ray diffraction.[12] The structure of the $[Rh(S,S\text{-chiraphos})(EAC)]^+$ ion, depicted in Figure 1, is essentially similar to that of **4**.[7] As in the latter case, the EAC substrate is coordinated

(6) Halpern, J.; Riley, D. P.; Chan. A. S. C.; Pluth, J. J. *J. Am. Chem. Soc.* **1977**, *99*, 8055.

(7) Chan. A. S. C.; Pluth, J. J.; Halpern, J. *Inorg. Chim. Acta* **1979**, *37*, L477.

(8) Chan. A. S. C.; Halpern, J. *J. Am. Chem. Soc.* **1980**, *102*, 838.

(9) In the case of the $[Rh(S,S\text{-chiraphos})S_2']^+$-catalyzed hydrogenation, the results reported here are for **1a** rather than **1b** as the substrate, since only in the case of **1a** was it possible to obtain single crystals of the adduct corresponding to **4** (i.e., of **7**) for an X-ray structure determination. However, the results of all the solution measurements (including the equilibrium constant, corresponding to k_3/k_{-3}, for the formation of the $[Rh(S,S\text{-chiraphos})(EAC)]^+$ and $[Rh(S,S\text{-chiraphos})(MAC)]^+$ adducts, the corresponding rate constants (k_4') for the reactions of the two adducts with H_2, as well as the various electronic and spectral parameters of the adducts) were virtually identical for **1a** and **1b**.

(10) Brown, J. M.; Chaloner, P. A. *Tetrahedron Lett.* **1978**, 1877.

(11) The slow rate of the step corresponding to eq 4 (i.e., the low value of k_4') precluded the interception at low temperatures of the *S,S*-chiraphos analogue of the subsequent intermediate **6**.

to the Rh atom through the oxygen atom of the amide carbonyl, as well as through normal symmetrical (η^2) coordination of the C=C bond. Together with the normal chelation of the *S,S*-chiraphos ligand, the overall coordination around the Rh atom thus corresponds to an idealized square-planar arrangement of ligands (C=C, O, 2P). Bond lengths and angles involving the Rh atom are essentially similar to those of **4** and are unexceptional.[7]

According to the generally accepted interpretation of the mechanistic scheme depicted by eq 3–6, addition of H_2 should occur to the Rh-coordinated face of the olefin in the Rh–olefin adduct. The *isolated* adduct **7** corresponds to coordination of the (C_α-*re*, C_β-*si*) face of EAC to the rhodium atom. Addition of H_2 to this face would yield *N*-acetyl-(*S*)-*phenylalanine ethyl ester* whereas the predominant product of reaction 1 (>95% enantiomeric excess) is the *R isomer*.

Three possible interpretations of this apparent discrepancy warrant consideration, namely: (1) The mechanism of hydrogenation is not that depicted by eq 3–6 but some other mechanism either which does not involve a catalyst–substrate adduct or in which H_2 addition occurs to the face of the olefin opposite to that coordinated to the Rh atom. (2) The isolated [Rh(*S,S*-chiraphos)(EAC)]$^+$ adduct **7**, whose structure is depicted in Figure 1, is the *minor* diastereomer in solution, whose concentration is too low to be detected, in equilibrium with the major diastereomer in which the opposite, i.e., (C_α-*si*, C_β-*re*), face of EAC is coordinated to Rh. (3) The isolated [Rh(*S,S*-chiraphos)(EAC)]$^+$ adduct **7** does correspond to the predominant diastereomer in solution, but the other diastereomer is sufficiently more reactive toward H_2 (corresponding to a sufficiently higher rate constant, k_4') that it dominates the enantioselectivity of the reaction.

We consider the first of the above alternatives unlikely because such a mechanistic pathway is essentially without precedent and because of the close parallels between the [Rh(*S,S*-chiraphos)S_2']$^+$-catalyzed hydrogenation and the corresponding [Rh(diphos)S_2']$^+$-catalyzed reaction for which the mechanism depicted by eq 3–6 (including the interception and characterization of the intermediates **4** and **6**) has been convincingly demonstrated.[7,8] The second alternative also seems to us unlikely in view of the absence of corroborative evidence and since examination of space-filling (CPK) models, while admittedly of limited reliability, does suggest that the structure of the isolated adduct **7** (Figure 1) is favored on steric grounds (and, hence, likely to be preferred also in solution) compared with that of the alternative diastereomer.

Support for the third of the above alternatives, which we favor, is provided by the fact that, although the structural and spectroscopic (electronic and NMR) properties of the predominant [Rh(*S,S*-chiraphos)(EAC)]$^+$ diastereomer are very similar to those of the [Rh(diphos)(MAC)]$^+$ analogue (**4**), its apparent reactivity toward H_2 (i.e., k_4') is only about $^1/_{60}$ that of the latter (i.e., k_4). On the other hand, the reactivity toward H_2 of the [Rh(*S,S*-chiraphos)]$^+$ adduct of an *achiral* olefin, i.e., 1-hexene, was actually found to be *higher* than that of the corresponding adduct of [Rh(diphos)]$^+$ (1.3×10^2 vs. 0.5×10^2 M^{-1} s^{-1}, respectively, at 25 °C). This suggests that the low value of k_4', relative to k_4, is due not to the intrinsically lower reactivity of the *S,S*-chiraphos-derived catalyst but rather to the low concentration of the "reactive" diastereomer of the EAC adduct. The origin of the reactivity difference of the two [Rh(*S,S*-chiraphos)(EAC)]$^+$ diastereomers presumably is associated with the relative stabilities of the resulting [RhH_2(*S,S*-chiraphos)(EAC)]$^+$ oxidative adducts. Examination of CPK models suggests that coordination of EAC to Rh through the (C_α-*si*, C_β-*re*) face does indeed give rise to the sterically favored diastereomer of the H_2 oxidative adduct. Following the usual migratory insertion-reductive elimination sequence, this diastereomer (derived from the minor diastereomer of **7**) would yield the observed R isomer of *N*-acetylphenylalanine ethyl ester.

We are thus led to the conclusion that at least for the systems we have examined, contrary to some earlier suggestions,[10,14–17] it is not the preferred mode of binding of the prochiral olefinic substrate to the catalyst (i.e., the step corresponding to eq 3) but rather differences in the rates of subsequent reaction of the diastereomeric catalyst–substrate adducts (i.e., of the step corresponding to eq 4) that determine the enantioselectivity in the asymmetric catalytic hydrogenation of the prochiral olefin.

It is noteworthy that, according to this interpretation, the reversibility of the initial catalyst–olefin adduct formation step (eq 3) should be reduced by increasing the rate of the subsequent H_2 oxidative addition step (eq 4). Thus, at sufficiently high H_2 concentrations (i.e., when $k_4[H_2][\mathbf{4}] \gg k_{-3}[\mathbf{4}]$), the rate and stereochemistry of the reaction should become determined by the initial binding of the prochiral olefinic substrate to the catalyst. For systems of the type we have described, this predicts that the enantioselectivity should decrease, with the possibility of eventual reversal of the stereochemistry, with increasing H_2 pressure. We propose this as the origin of the inverse dependence of optical yield on the H_2 partial pressure which has been reported for several related catalyst systems,[1,4,18] and for which a convincing explanation has not previously been advanced. The widespread observation of such an inverse dependence of optical yield on the H_2 partial pressure suggests that our conclusion concerning the origin of enantioselectivity in such catalyst systems may be quite general.[19]

Acknowledgments. We gratefully acknowledge support of this research by the National Science Foundation, generous gifts of *S,S*-chiraphos from Drs. B. Bosnich and M. D. Fryzuk, and a generous loan of rhodium from Engelhard Industries. The NMR facilities used in this research were supported in part through the University of Chicago Cancer Center Grant NIH-CA-14599.

(12) Orange-red crystals of [Rh(*S,S*-chiraphos)(EAC)]ClO_4 were grown by diffusing ether into a methanol solution of the salt. The X-ray analysis was performed on a crystal of approximate dimensions 0.263 × 0.278 × 0.023 mm, using a Picker FACS-1 diffractometer equipped with Mo Kα radiation (0.71069 Å) and a graphite monochromator. *Crystal data*: Space group, $P2_1$; a = 10.725 (2), b = 19.286 (6), c = 11.708 (2) Å, β = 122.77 (1)°; Z = 2; ρ_{calcd} = 1.415 g cm^{-3}; ρ_{obsd} = 1.38 g cm^{-3}. A total of 3590 diffractions (sin θ/λ = 0.59) were collected, of which 3380 with $F \geq 2\sigma(F)$ were used in the refinement. No significant intensity changes were observed during the data collection. The structure was solved by Patterson methods with full-matrix least-square refinement by using un-ionized scattering factors and treating the phenyl groups as rigid bodies (with 1.395-Å C–C bond lengths) and the H atoms as fixed contributions (with 1.08-Å C–H bond lengths and normal geometries), except for the N-bonded H atom which was neglected. Anisotropic thermal parameters were used for the other atoms. The refinement led to final values of R = 0.046, R_w = 0.045, and S = 1.2. The absolute configuration of **7** was assigned on the basis of the known absolute configuration of the *S,S*-chiraphos ligand and was consistent with the assignment based on the *R*-factor ratio test[13] since fitting the data to the opposite configuration yielded R = 0.047, R_w = 0.046 and S = 1.2.

(13) Hamilton, W. C. *Acta Crystallogr.* **1965**, *18*, 502.
(14) Brown, J. M.; Chaloner, P. A. *J. Chem. Soc., Chem. Commun.* **1978**, 321.
(15) Pino, P.; Consiglio, G. In "Fundamental Research In Homogeneous Catalysis;" Tsutsui, M., Ed.; Plenum Press: New York, 1979; Vol. 3, p 519.
(16) Ojima, I.; Kogure, T. *Chem. Lett.* **1978**, 1175.
(17) Ojima, I.; Kogure, T. *Chem. Lett.* **1979**, 641.
(18) Ojima, I.; Kogure, T.; Yoda, N. *Chem. Lett.* **1979**, 495.
(19) Note Added in Proof: In a communication that appeared subsequent to submission of this manuscript, Brown and Chaloner[20] report that in the case of the α-benzamidocinnamic acid adduct of [(*R,R*)-1,2-bis(*o*-methoxyphenylphenylphosphino)ethanerhodium(I)]$^+$, where both diastereomers corresponding to **4** can be detected by NMR in solution, H_2 reacts selectively with the *minor* diastereomer at low temperatures (−53 °C) to form a hydridoalkylrhodium complex analogous to **6**. This is consistent with, and provides additional support for, our conclusion.
(20) Brown, J. M.; Chaloner, P. A. *J. Chem. Soc., Chem. Commun.* **1980**, 344.

A. S. C. Chan, J. J. Pluth, Jack Halpern*
Department of Chemistry, The University of Chicago
Chicago, Illinois 60637
Received April 15, 1980